BIOCHEMISTRY
including biophysical chemistry & molecular biology

ARTICLE

pubs.acs.org/biochemistry

The Conformational Flexibility of the Helicase-like Domain from *Thermotoga maritima* Reverse Gyrase Is Restricted by the Topoisomerase Domain

Yoandris del Toro Duany,[†] Dagmar Klostermeier,[*,†,‡] and Markus G. Rudolph[§]

[†]Biozentrum, Department of Biophysical Chemistry, University of Basel, Klingelbergstrasse 70, CH-4056 Basel, Switzerland

[‡]Institute for Physical Chemistry, University of Muenster, Correnssstrasse 30, D-48149 Muenster, Germany

[§]Hoffmann-La Roche AG, Grenzacher Strasse 124, CH-4070 Basel, Switzerland

Supporting Information

ABSTRACT: Reverse gyrase is the only enzyme known to introduce positive supercoils into DNA. Positive supercoiling is achieved by the functional cooperation of a helicase-like and a topoisomerase domain. The isolated helicase-like domain is a DNA-stimulated ATPase, and the isolated topoisomerase domain can relax supercoiled DNA. In the context of reverse gyrase, these individual activities are suppressed or attenuated. The helicase-like domain of *Thermotoga maritima* reverse gyrase is a nucleotide-dependent conformational switch that binds DNA and ATP cooperatively. It provides a nucleotide-dependent DNA-binding site to reverse gyrase and thus serves as a valuable model for the investigation of the effect of nucleotides on DNA processing by reverse gyrase that is key to its supercoiling activity. To improve our understanding of the structural basis for the functional cooperation of a helicase domain with a DNA topoisomerase, we have determined the structures of the isolated helicase-like domain of *T. maritima* reverse gyrase in five different conformations. Comparison of these structures reveals extensive domain flexibility in the absence of conformational restrictions by the topoisomerase that is consistent with single-molecule Förster resonance energy transfer experiments presented here. The structure of the first ADP-bound form provides novel details about nucleotide binding to reverse gyrase. It demonstrates that reverse gyrases use the canonical nucleotide binding mode common to superfamily 2 helicases despite large deviations in the conserved motifs. A characteristic insert region adopts drastically different structures in different reverse gyrases. Counterparts of this insert region are located at very different positions in other DNA-processing enzymes but may point toward a general role in DNA strand separation.

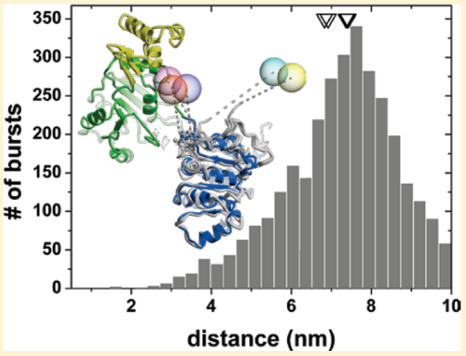

The degree of DNA supercoiling affects central cellular processes such as replication, recombination, and repair.[1] It is regulated by DNA topoisomerases, an enzyme class that catalyzes the interconversion of different topoisomers. Bacterial gyrases introduce negative supercoils in an ATP-dependent process[2] and thereby relieve topological stress ahead of the replication fork. Reverse gyrases catalyze the inverse reaction, namely the introduction of positive supercoils into DNA, in an ATP-dependent fashion. These enzymes are unique to thermophiles and hyperthermophiles where they are thought to exert protective functions for DNA at high temperatures.[3,4] Reverse gyrases share a unique modular structure that combines an N-terminal helicase-like domain with a C-terminal topoisomerase domain.[5] The topoisomerase domain is homologous to prokaryotic and eukaryotic type IA DNA topoisomerases. It has been shown to relax negatively supercoiled DNA in vitro,[6] but this activity is suppressed in reverse gyrase. The helicase-like domain is divided into two subdomains, termed H1 and H2, that both bear similarity to the RecA fold[7] (Figure 1A). H1 and H2 harbor the signature motifs of superfamily 2 (SF2) helicases necessary for ATP and DNA binding, though their sequences substantially differ from the SF2 consensus.[7] The critical role of the helicase-like domain for reverse gyrase activity has been demonstrated by the deleterious effect of mutations in the helicase motifs.[8] The so-called latch domain (Figure 1A), an insertion in H2, allows for communication between the helicase and topoisomerase domains.[9,10] The latch is required for positive DNA supercoiling by *Thermotoga maritima* reverse gyrase, but not for nucleotide binding and hydrolysis.[10]

The helicase-like domain of *T. maritima* reverse gyrase is a nucleotide-dependent conformational switch that binds DNA and ATP with positive cooperativity[11,12] and provides a nucleotide-dependent DNA-binding site to reverse gyrase. The DNA binding properties of the different nucleotide states are masked in the context of reverse gyrase because of additional DNA binding sites.[10,11] The isolated helicase-like domain thus serves as a valuable model for investigation of the effect of nucleotides on

Received: February 15, 2011
Revised: May 10, 2011
Published: June 01, 2011

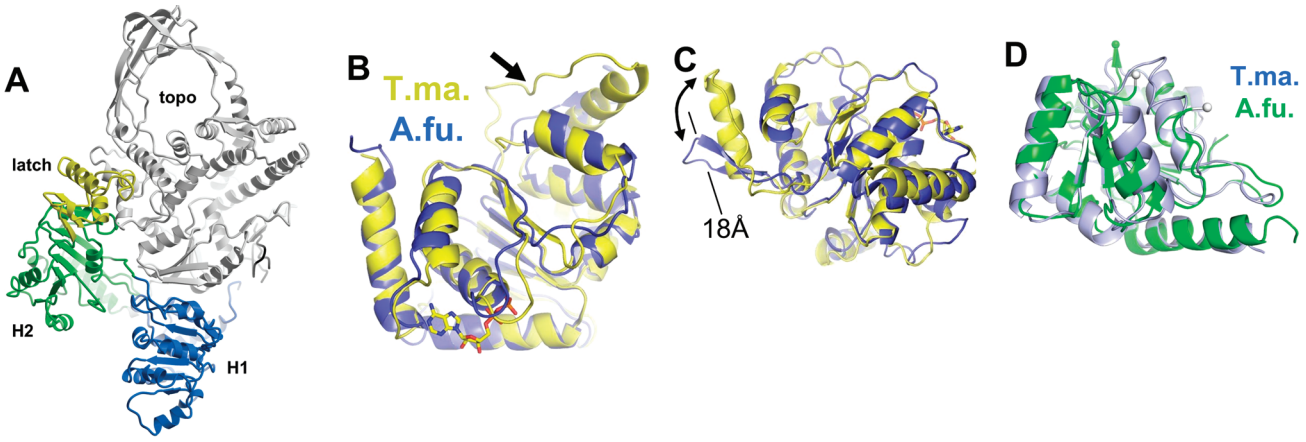

Figure 1. Overview of reverse gyrase. (A) Structure of reverse gyrase from *A. fulgidus* (PDB entry 1GKU). The topoisomerase domain is colored gray. The helicase-like domain is composed of the two RecA-like subdomains H1 (blue) and H2 (green). The latch domain (yellow) is inserted in H2 and allows communication between the helicase and topoisomerase domains. In this study, the isolated helicase-like domain without the latch (rgyr_hel_Δlatch) is used to assess domain flexibility and nucleotide binding. (B) Superposition of H1 of *T. maritima* rgyr_hel_Δlatch (yellow) and *A. fulgidus* (blue) reverse gyrase. The arrow denotes an insert region that varies strongly in sequence length. In *A. fulgidus*, this region forms a β-hairpin, but in *T. maritima*, it is an α-helix−loop motif. (C) View rotated ∼90° about the *z*-axis relative to panel B highlighting the strong deviation of the insert regions. (D) Superposition of H2. *A. fulgidus* reverse gyrase (green) depicted without the latch region (normally inserted at the green sphere). The gray spheres denote a disordered loop in *A. fulgidus* reverse gyrase that could be traced in the *T. maritima* enzyme (blue).

DNA processing by reverse gyrase that is at the heart of its positive supercoiling activity.

The structures of *Archaeoglobus fulgidus* reverse gyrase in the apo and ADPNP-bound forms[7] are the only structural information on reverse gyrases to date. To provide a structural basis for understanding the cooperation of the helicase-like domain with the topoisomerase domain in positive supercoiling, we determined the crystal structure of the helicase-like domain of *T. maritima* reverse gyrase, an enzyme that has been extensively characterized biochemically.[10−13] Three crystal structures with five different conformations of the *T. maritima* reverse gyrase helicase-like domain without the latch domain (rgyr_hel_Δlatch) show large variations in H1 and H2 domain juxtaposition, consistent with single-molecule Förster resonance energy transfer (FRET) experiments.[12] Interestingly, the different conformations cluster around two preferred conformations, none of which resembles the conformation imposed by the topoisomerase domain in full-length reverse gyrase. The structure of the ADP−Mg^{2+} complex of rgyr_hel_Δlatch reveals significant differences and novel features compared to the *A. fulgidus* reverse gyrase−ADPNP complex and offers new insight into the functional communication between SF2 motifs in reverse gyrases. An insert region that has counterparts in other DNA-processing enzymes can adopt very different structures among reverse gyrases and may play an important role in DNA strand separation.

MATERIALS AND METHODS

The helicase-like domain lacking the latch (rgyr_hel_Δlatch) was constructed and purified as described in detail in ref 10. Three diffraction-quality crystal forms for rgyr_hel_Δlatch were obtained at 25 °C using the sitting drop vapor diffusion setup by 1:1 (v/v) mixing of 20 mg/mL protein in 50 mM Tris-HCl (pH 7.5), 0.2 M NaCl, 10 mM $MgCl_2$, 10 mM $Zn(OAc)_2$, and 2 mM β-mercaptoethanol with reservoir solutions consisting of 0.2 M magnesium formate and 20% PEG 3350 (PDB entry 3OIY), 0.2 M Li_2SO_4 and 20% PEG 3350 (PDB entry 3P4X), and 0.1 M HEPES-NaOH (pH 7.5) and 30% PEG 300 (PDB entry 3P4Y). Crystals were cryo-protected with paraffin oil, mounted in an arbitrary orientation, and data were collected at Swiss Light Source beamlines PX-II and PX-III. Intensities were integrated with XDS[14] and scaled with SCALA (PDB entries 3P4X and 3OIY)[15] or SADABS (PDB entry 3P4Y; Bruker). Systematic absences identified space group $P2_12_12_1$ for two nonisomorphous data sets representing apo and ADP-bound structures (two molecules per asymmetric unit), and rare space group *P*2 for a third crystal form (one molecule per asymmetric unit). Phasing and refinement of the apo-$P2_12_12_1$ form (PDB entry 3OIY) were described previously,[10] and the H1 and H2 domains of this structure were used as search models for phasing of the other two data sets by molecular replacement using PHASER.[16] Models were built in COOT[17] and refined with PHENIX[18] using separate TLS descriptions for the H1 and H2 domains. Data collection and refinement statistics are listed in Table 1. The coordinates and structure factors have been deposited in the Protein Data Bank (PDB) (entries 3OIY, 3P4X, and 3P4Y). Figures were created with Bobscript,[19] Raster3D,[20] Pymol (http://www.pymol.org), and ESPript.[21] Single-molecule FRET experiments were performed with rgyr_hel_Δlatch_S169C/F332C labeled with AlexaFluor 488 (donor) and tetramethylrhodamine (acceptor) using a home-built confocal microscope.[22,23] The labeled protein exhibited DNA-stimulated ATPase activity similar to that of the wild type. ATPase hydrolysis was monitored in a coupled enzymatic assay as described previously.[13] FRET data analysis was performed as described previously.[23,24]

RESULTS

Crystals of the helicase-like domain including the latch were obtained but did not diffract X-rays. The latch does not affect the intrinsic ATPase activity of the helicase-like domain and has little effect on nucleotide affinity.[10] A latch deletion mutant (rgyr_hel_Δlatch) still shows DNA-stimulated ATPase activity and thus constitutes a valid model for structural studies. This construct

Table 1. Data Collection, Phasing, and Refinement Statistics

	apo, 3OIY[a]	ADP complex, 3P4X	apo, 3P4Y
	Data Collection		
resolution range (Å)[b]	132.7−2.35 (2.44−2.35)	129.7−2.4 (2.5−2.4)	48.8−3.20 (3.3−3.2)
space group	$P2_12_12_1$	$P2_12_12_1$	$P2$
cell dimensions	a = 59.6 Å, b = 126.5 Å, c = 132.7 Å	a = 59.2 Å, b = 111.2 Å, c = 129.7 Å	a = 61.9 Å, b = 59.2 Å, c = 67.7 Å, β = 98.2°
no. of unique reflections[b]	42547 (4453)	34066 (3511)	7475 (376)
multiplicity[b]	7.1 (7.4)	3.6 (3.7)	3.4 (3.7)
completeness (%)[b]	99.6 (100)	99.1 (99.9)	91.4 (99.9)
R_{sym} (%)[b,c]	9.9 (65.9)	6.4 (63.5)	17.5 (65.6)
average $\langle I/\sigma(I)\rangle$[b,c]	9.7 (1.3)	12.0 (1.1)	7.2 (1.6)
	Refinement		
resolution range (Å)[b]	44.4−2.35 (2.41−2.35)	56.0−2.4 (2.5−2.4)	44.3−3.2 (4.0−3.2)
R_{cryst} (%)[b,d]	20.8 (39.4)	18.6 (32.7)	28.6 (33.0)
R_{free} (%)[b,d]	25.1 (41.5)	25.6 (41.4)	29.7 (34.8)
no. of residues/waters	807/99	809/52	407/0
phase error/coordinate error[e]	28.3°/0.38 Å	29.3°/0.36 Å	33.2°/0.49 Å
rmsd for bonds/angles	0.012 Å/1.56°	0.009 Å/1.14°	0.003 Å/0.54°
Ramachandran plot (%)[f]	96.8/3.1/0.1	91.7/8.0/0/0.3	89.4/10.1/0.3/0.3

[a] Data reproduced from ref 10. [b] Values in parentheses correspond to those of the highest-resolution shell. [c] Calculated with XPREP (Bruker). [d] $R_{cryst} = \Sigma||F_o| - |F_c||/\Sigma|F_o|$, where F_o and F_c are the structure factor amplitudes from the data and the model, respectively. R_{free}[41] is R_{cryst} with 5% of the test set structure factors. [e] Based on maximum likelihood after refinement with PHENIX.[18] [f] Calculated using PROCHECK.[42] Numbers reflect the percentage amino acid residues of the core, allowed, additionally allowed, and disallowed regions, respectively.

crystallizes readily, suggesting that the latch may be only loosely connected to H2, consistent with its previously suggested flexibility.[7] Three crystal structures of rgyr_hel_Δlatch were obtained and refined to resolutions of 2.35, 2.4, and 3.2 Å. The structures comprise five independent molecules and provide higher-resolution information about this part of reverse gyrase than what was previously available.

Comparison of *A. fulgidus* and *T. maritima* Subdomains H1 and H2. The core structures of H1 and H2 resemble RecA folds, i.e., a central parallel β-sheet flanked by α-helices on both sides. The H1 domains of *T. maritima* and *A. fulgidus* reverse gyrases superpose with a root-mean-square deviation (rmsd) of 1.8 Å over 187 residues (43% sequence identity). Similarly, the H2 domains superpose with an rmsd of 1.6 Å over 166 residues (39% identical sequences). Notably, an insertion is present in the sequence of *T. maritima* reverse gyrase compared to *A. fulgidus* (Figure S1 of the Supporting Information). At residue Gly239 of H1, 12 residues are inserted and form a loop region (arrow in Figure 1B). This loop and its preceding α-helix form a lid-like structure. In contrast, the corresponding region in *A. fulgidus* reverse gyrase forms a small, two-stranded β-sheet (Figure 1C). In a superposition of the H2 structures, the tips of these structural elements are ∼18 Å from each other (Figure 1C). The sequence of this insertion is quite variable among reverse gyrases, and it may comprise up to 41 residues (Figure S2 of the Supporting Information).

Within the RecA fold of H2 (Figure 1D), the latch domain is inserted at residue Gly389. This domain is present in all reverse gyrases but also varies strongly in both extent and sequence (Figure S2 of the Supporting Information). Comparison of the H2 structures from *A. fulgidus* and *T. maritima* reveals that the deletion of the latch region does not alter the fold of H2.[10]

Flexibility of the Helicase-like Domain. The helicase-like domain is formed by H1 and H2 that are connected by a linker sequence, which spans residues 280−286 in *T. maritima* reverse gyrase. While H2 follows the classic RecA topology with a seven-stranded β-sheet, H1 has only six β-strands. The seventh β-strand, normally formed by parts of the H1−H2 linker region, is not present because of the large displacements of H2 relative to H1. The same topology is present in the *A. fulgidus* enzyme.[7]

In the absence of interactions with the topoisomerase domain, H1 and H2 in rgyr_hel_Δlatch engage in only a few contacts, and the flexible linker allows the relative juxtapositions of H1 and H2 to vary strongly (Figure 2A). No common pattern of H1−H2 interactions is evident, strongly indicating that these modules are conformationally independent in the absence of DNA or the topoisomerase domain. Similarly, in both available structures of *A. fulgidus* reverse gyrase, H1 and H2 are connected by only five hydrogen bonds (different compared to rgyr_hel_Δlatch), and the buried surface area between them covers a mere 430 Å^2. In contrast, the topoisomerase domain interacts extensively with H1 and H2, fixing them in space.

None of the five conformations observed in the rgyr_hel_Δlatch crystal structures represents that of the helicase-like domain in *A. fulgidus* reverse gyrase or compares to the closed conformation of DEAD box helicases in complex with RNA and an ATP analogue, such as Vasa (gray sphere in Figure 2B). However, as reverse gyrase does belong to SF2 but is not a DEAD box protein, a direct comparison with Vasa may not be possible. The location of H2 with respect to H1 is not random but forms two clusters (Figure 2B). Single-molecule FRET experiments with rgyr_hel_Δlatch labeled at cysteines introduced at positions 169 and 332 reveal a mean distance between donor and acceptor dyes of 7.5 nm (Figure 2C,D). The corresponding Cβ−Cβ distances in the crystal structures vary between 6.8 and 7.4 nm, a strong indication that the conformations trapped in the crystal lattice represent conformations that are predominantly populated

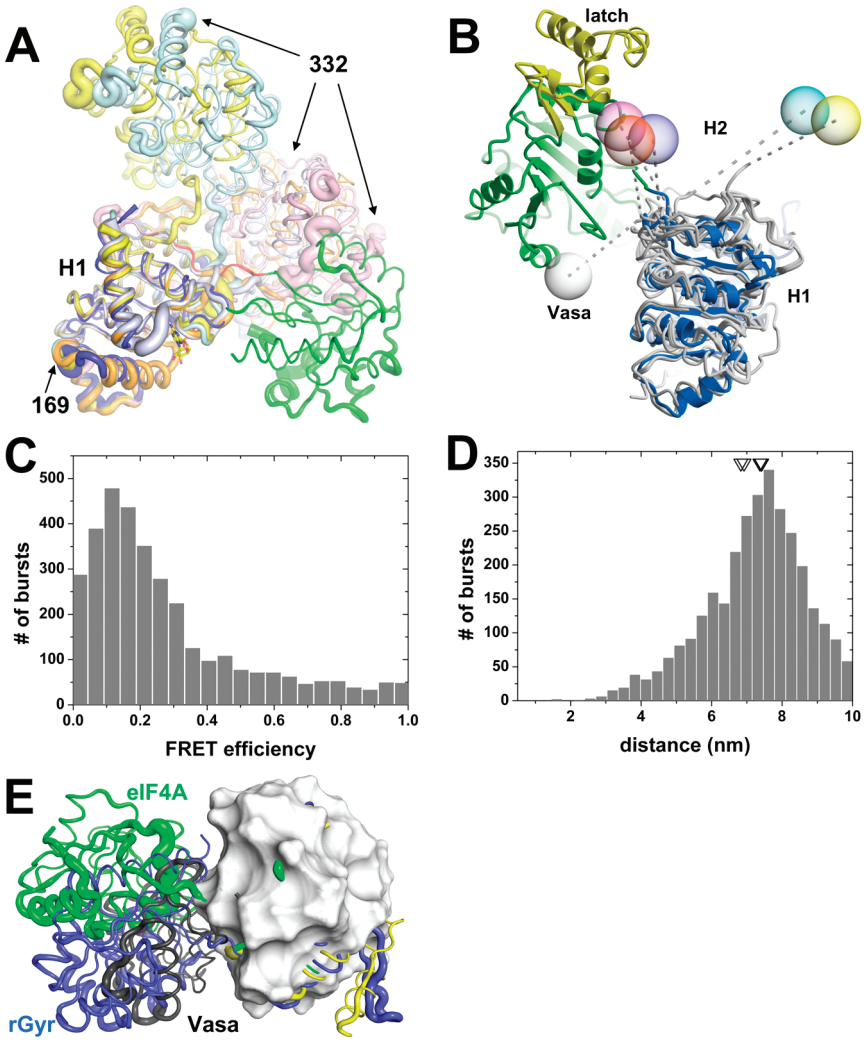

Figure 2. Large domain flexibility in rgyr_hel_Δlatch and comparison with related structures. (A) Superposition of the five different *T. maritima* rgyr_hel_Δlatch conformations onto H1 of *A. fulgidus* reverse gyrase. The location of H2 varies widely because of the lacking restraint by the topoisomerase domain. H2 of *A. fulgidus* reverse gyrase is colored green as a reference. *T. maritima* H2 domains are colored yellow and blue (molecules 1 and 2 of PDB entry 3OIY), cyan and orange (molecules 1 and 2 of PDB entry 3P4X), and pink (PDB entry 3P4Y). Cysteine positions 169 and 332 for fluorescent labeling in FRET experiments are indicated. (B) View rotated 180° about the *y*-axis relative to panel A. The centers of mass of the H2 domains are shown as transparent spheres colored the same as in panel A. Dashed lines connect the centers to the C-termini of H1. The five conformations of rgyr_hel_Δlatch form two clusters. The closed form of the DEAD box RNA helicase Vasa is shown as a gray sphere. This structure is only adopted when RNA and ATP are present. (C) Single-molecule FRET histogram for rgyr_hel_Δlatch (S169C/F332C), labeled with AlexaFluor 488 (donor) and tetramethylrhodamine (acceptor). The mean FRET efficiency is ~0.1. (D) Distance histogram calculated from the data in panel C. The predominant distance between donor and acceptor dyes is 7.5 nm. The empty triangles indicate the Cβ−Cβ distances between the labeled Cys169 and Cys332 residues in the five different structures (PDB entry 3OIY, 7.4 and 6.8 nm; PDB entry 3P4X, 7.4 and 6.9 nm; PDB entry 3P4Y, 7.4 nm) and compare favorably with the mean dye distance in solution. (E) Comparison of the H2 locations of *A. fulgidus* reverse gyrase (blue) with the closed form of Vasa (gray) and the open form of eukaryotic translation initiation factor eIF4A (green) shows large domain movements of the helicase cores. The structures were superposed on H1. The surface of Vasa H1 is shown, highlighting the protruding insert regions unique to reverse gyrases (yellow for *T. maritima* and blue for *A. fulgidus* reverse gyrase).

in solution. rgyr_hel_Δlatch exhibits DNA-stimulated ATPase activity,[10] which shows that DNA can align H1 and H2 for ATP hydrolysis in the absence of the topoisomerase domain. The conformational restriction of H1 and H2 by the topoisomerase domain is inhibitory with respect to ATP hydrolysis but is likely to support reverse gyrase activity. Interestingly, the helicase core of *A. fulgidus* reverse gyrase adopts an intermediate state between closed (Vasa) and open (rgyr_hel_Δlatch). A half-open conformation is also documented for the eIF4A−eIF4G complex[25] (Figure 2E).

Nucleotide Binding to the H1 Domain. The helicase-like domain is responsible for ATP binding and hydrolysis.[11] Although all crystallization setups were performed with ADPNP and Mg^{2+}, only in one instance (PDB entry 3P4X) was a nucleotide observed in the electron density that was assigned as ADP. The affinity of rgyr_hel_Δlatch for ADP is ~5.5-fold higher than for ADPNP,[10] and ADP generated from ADPNP by limited hydrolysis or introduced as an impurity will be preferentially bound. The nucleotide exclusively interacts with H1, forming a total of 11 hydrogen bonds with the adenine base and the diphosphate

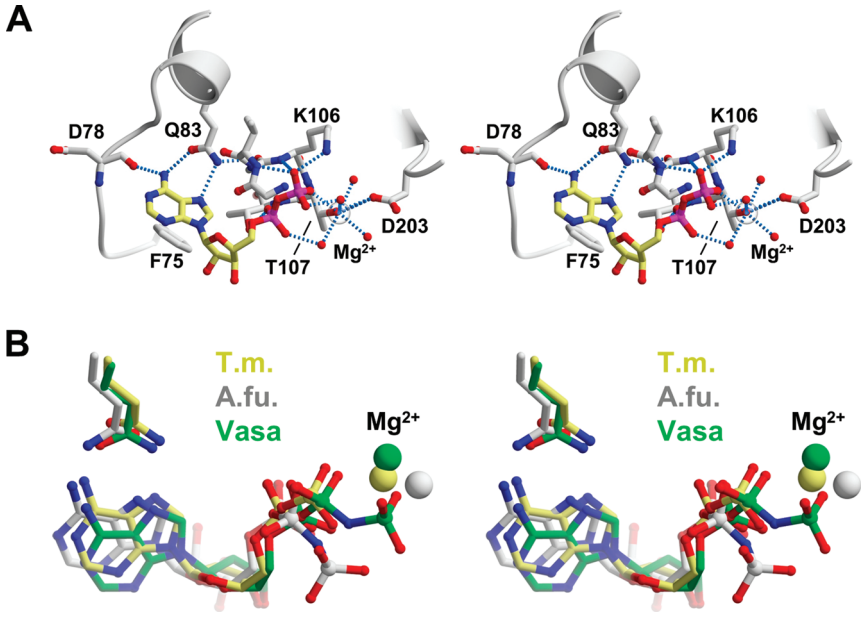

Figure 3. Detailed view of nucleotide binding to reverse gyrase. (A) Stereo figure of the hydrogen bond network of ADP and Mg^{2+} bound to *T. maritima* reverse gyrase. The adenine base is bound by three hydrogen bonds (dashed lines) to the conserved Gln83 of the Q-motif and the backbone carbonyl group of Asp78. A hydrophobic sandwich is formed between adenine and Phe75. The β-phosphate forms hydrogen bonds to the P-loop, and its charge is neutralized by Lys106 and the Mg^{2+}—aquo complex. Mg^{2+} connects the nucleotide with Asp203 of the DDVD motif, a modified DEAD box that is conserved in RNA helicases. (B) Comparison of the nucleotide binding modes of *T. maritima* and *A. fulgidus* reverse gyrases with the DExD/H-helicase Vasa. Mg^{2+} ions are shown as spheres. Note the deviation of the γ-phosphate in *A. fulgidus* reverse gyrase compared to that in Vasa, leading to the absence of interactions with the Mg^{2+} ion.

moiety (Figure 3). Thus, ADP binding will not affect H1—H2 domain flexibility (see above). The ribose is not involved in any interactions with the protein. The lack of interactions with the 2′-OH group of the ribose rationalizes the previous observation that 2′-desoxy-ATP is also accepted as a substrate of *A. fulgidus* reverse gyrase,[9] and the observation that mantADP is a suitable analogue for monitoring adenine nucleotide binding to *T. maritima* reverse gyrase.[11,13] Thus, ribose-modified nucleotides should bind to reverse gyrases in general.

In contrast to the ribose moiety, the adenine base is recognized specifically by a region that bears homology to the Q-motif in DEAD box proteins, consisting of a conserved glutamine residue and a hydrophobic (often aromatic) side chain located 13 residues upstream of the glutamine.[26,27] Such a glutamine is conserved in reverse gyrases, discriminating adenine from other nucleobases via two hydrogen bonds (Figure 3A). A third hydrogen bond is formed between the exocyclic N6 atom of adenine and the main chain carbonyl group of Asp78. The interaction network with adenine is completed by hydrophobic contacts with Phe75 (Val54 in *A. fulgidus* reverse gyrase). This adenine-specific pocket stands in contrast to the observation that *A. fulgidus* reverse gyrase, although preferring ATP, can apparently use all four standard NTPs and dNTP as substrates.[9]

The α- and β-phosphate moieties form hydrogen bonds to the main chain amide nitrogen atoms of P-loop residues Gly103, Gly105, Lys106, Thr107, and Thr108. The charge of the β-phosphate is neutralized by Lys106 and a Mg^{2+} ion. This Mg^{2+} ion is directly bound to the β-phosphate and coordinated octahedrally by the side chain of Thr107 and four water molecules. In DEAD box helicases, the nucleotide-bound Mg^{2+} ion connects the P-loop with the first aspartate residue of the DEAD box. Reverse gyrases possess a modified DEAD box, the DDVD motif, where the valine may also be Ala, Ile, or Ser. Similar to DEAD box proteins, the Mg^{2+}—aquo complex in *T. maritima* rgyr_hel_Δlatch connects the nucleotide with the first aspartate (Asp203) of the DDVD motif. An equivalent interaction is present in the closed exon junction complex[28,29] but absent in DDX19[30] and Vasa.[31] A second link between the P-loop and the DDVD motif is established by a direct hydrogen bond of the Thr107 and Asp203 side chains (Figure 3A). Again, this interaction is present in the exon junction complex but absent in the currently available closed DEAD box helicase structures.

To date, only one other reverse gyrase—nucleotide complex structure is available. In the ADPNP complex of *A. fulgidus* reverse gyrase (PDB entry 1GL9), a minor error is a 180° rotated carboxamide side chain of the conserved glutamine, and the C2 epimeric arabinose was built instead of a ribose[7] (Figure 3B). The P-loops of reverse gyrases adopt different conformations in the apo and nucleotide-bound forms. The Cα—Cα distance between Thr102 (*T. maritima*) and the equivalent Thr80 (*A. fulgidus*) is 5 Å in the apo forms and 2 Å in the nucleotide-bound forms. In both *T. maritima* and *A. fulgidus* reverse gyrase, the P-loop essentially collapsed onto the phosphate part of the nucleotide. Thus, the P-loop may be mobile in the apo form of reverse gyrases and becomes fixed only after nucleotide binding. The locations of the adenine, sugar moiety, and α-phosphate are roughly similar between the *T. maritima* and *A. fulgidus* nucleotide complexes. Large differences are apparent for the locations and coordination of the Mg^{2+} ions and the connection of the P-loop with the DDVD motif. In *T. maritima* rgyr_hel_Δlatch, Thr107 is a direct ligand for the Mg^{2+} ion and binds to Asp203 of the DDVD motif (Figure 3A). By contrast, the analogous Thr85 in *A. fulgidus* only contacts the β-phosphate and is too far from

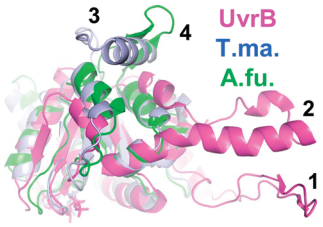

Figure 4. Insertions in UvrB and reverse gyrase helicase-like H2 domains. UvrB (PDB entry 1d9z, magenta) has two insertions (right part of the image) that might contribute to strand separation, a β-hairpin (1) and an α-helix connecting back to H2 via a loop region (2). The UvrB α-helix is located closer to the insertion in the reverse gyrase H2 domains (3 and 4) than the β-hairpin and is structurally similar to *T. maritima* H2 (light blue). Similar to UvrB, *A. fulgidus* reverse gyrase H2 (green) possesses a β-hairpin (4). However, the reverse gyrase insertions are located at very different sites in the H2 structure compared to the UvrB insertions, and their putative involvement in DNA strand separation is currently unconfirmed.

either the Mg^{2+} ion or the DDVD motif. In conclusion, the structures we report here establish that the salient features of nucleotide binding to DEAD box helicases, including the Q-motif, the P-loop, and the connection to the (modified) DEAD box, are present in *T. maritima* reverse gyrase.

DISCUSSION

In this study, the latch region had to be deleted from the *T. maritima* helicase-like domain to obtain diffracting crystals. The latch does not interact with any residues of the nucleotide binding pocket, and the mutant serves as a meaningful model system for nucleotide binding to *T. maritima* reverse gyrase. The fold of the H2 domain remains unaltered upon latch deletion.[10] Furthermore, H2 does not significantly interact with H1 in any of the reverse gyrase structures determined so far.

One of the larger sequence differences between *T. maritima* and *A. fulgidus* reverse gyrases is an insertion of 12 residues at position 240 (*T. maritima* numbering). This insertion effectively replaces a β-hairpin of *A. fulgidus* reverse gyrase with a long α-helix followed by a loop region (Figures 1B,C and 2E). For *A. fulgidus* reverse gyrase, a function of this β-hairpin for strand separation was hypothesized.[7] β-Hairpins that were implicated in strand separation are also present in the H1 domain of SF2 helicases NS3[32] and Hel308[33] and in the SF1 excision repair nuclease UvrB,[34] albeit at quite different locations in the structures. Interestingly, another insertion close to those observed in H1 of *T. maritima* and *A. fulgidus* reverse gyrases is present in UvrB (Figure 4). This insertion adopts a shape similar to that of the insertion in *T. maritima* reverse gyrase, namely a long α-helix that connects back to H1 via a loop region. A multiple-sequence comparison of 19 reverse gyrases (Figure S2 of the Supporting Information) demonstrates that *A. fulgidus* harbors an exceptionally compact reverse gyrase. The insertion in *T. maritima* is the smallest of the set but can comprise up to 42 residues (*Pyrococcus kodakaraensis*, with all pyrococci having >38-residue insertions). Thus, if this region should participate in strand separation, and if the insertion in UvrB has an equivalent function, the task can be achieved not only via very different sequence lengths but also via very different structures. Alternatively, the insertion might undergo a helix loop to β-hairpin transition during catalysis. Whether insertions at this position constitute a general feature of DNA and DExD/H helicases that is involved in nucleic acid strand separation remains to be determined.

While the general features of nucleotide binding to reverse gyrases and DEAD box helicases are the same with the adenine base binding to the Q-motif and the phosphate moiety located in the P-loop, the details of nucleotide binding in reverse gyrases differ from those observed in DEAD box helicases. In the structure of rgyr_hel_Δlatch, Thr107 is a direct Mg^{2+} ligand, a pattern often encountered in P-loop-containing proteins. For example, in the GTP-binding protein Ras, Ser17 of the P-loop binds to the Mg^{2+} ion.[35] With DEAD box and related helicases, the picture is somewhat incoherent. In the human DDX19—ADPNP—RNA complex,[30] the threonine at this position does not interact directly with Mg^{2+}, and in the *Drosophila* Vasa—ADPNP—RNA complex,[31] the interaction is indirectly mediated by a water molecule. By contrast, a direct interaction of the threonine with Mg^{2+} is present in the RNA-bound exon junction complex with either ADPNP[28] or the transition state analogue ADP-AlF_3.[29] All of these complexes are regarded as closed structures, trapped either in a state prior to RNA unwinding or after release of the first strand.

Superposition of the ADP—Mg^{2+} complex with that of closed-form DEAD box helicases predicts a likely position for the γ-phosphate in a reverse gyrase—ATP complex (Figure 3B). The γ-phosphate should follow the extended conformation present in the ATP analogue of the Vasa helicase,[31] and the Mg^{2+} ion should be bound to both the β- and γ-phosphate. Instead, neither the β-phosphate nor the γ-phosphate of the ADPNP in the *A. fulgidus* reverse gyrase structure interacts with Mg^{2+}, but the γ-phosphate takes a very different path pointing into the solvent (Figure 3B).

The helicase-like domain of reverse gyrase is composed of the H1 and H2 domains and resembles the helicase core of DEAD box proteins. An essential feature of these helicases is a bipartite nucleic acid binding site that is generated by both RecA-like domains[31] (reviewed in ref 36). Generation of this binding site requires closure of the interdomain cleft, which also harbors the nucleotide binding site.[28,30,31,37] DEAD box helicases and reverse gyrases share several common denominators. First, the spatial distribution of conserved motifs is similar.[7] Second, mutational studies defined important contributions of these motifs to supercoiling.[8] Third, cooperativity exists between DNA and ATP binding in the helicase-like domain of *T. maritima* reverse gyrase.[11] Fourth, several crystal structures of DEAD box helicases in the absence of either RNA and ATP analogues have shown a plethora of open conformations where the N- and C-terminal RecA-like domains are splayed apart[28,38−40] (unpublished observations, PDB entry 2Z0M). Binding of nucleotide alone does not induce a closure of the cleft between H1 and H2, not in the intact *A. fulgidus* reverse gyrase[7] or in the *T. maritima* rgyr_hel_Δlatch variant (this work), and also not in DEAD box proteins.[22] Taken together, these data suggest similar concerted conformational changes for the helicase domains of reverse gyrase and DEAD box helicases upon ATP and nucleic acid binding. Indeed, single-molecule FRET studies of the isolated reverse gyrase helicase-like domain demonstrate a closure upon nucleotide and DNA binding.[12]

In *T. maritima* reverse gyrase, binding of DNA and nucleotide is less cooperative than in the isolated helicase-like domain, pointing toward an inhibitory effect of the topoisomerase domain for the required closure of the helicase-like domain.[11] It is therefore conceivable that both nucleotide and DNA binding

are required to alleviate the conformational restrictions imposed on the helicase-like domain by the topoisomerase domain of reverse gyrase. Likewise, nucleotide hydrolysis by the helicase-like domain is attenuated by the topoisomerase domain in reverse gyrase. The activation of eukaryotic initiation factor eIF4A by eIF4G through the stabilization of a half-open conformation demonstrates that a balance of conformational restriction and conformational plasticity is crucial for DEAD box protein function.[24] Possibly, restriction by the topoisomerase domain impedes rapid alternation between open and closed forms of H1 and H2. In the isolated *T. maritima* helicase-like domain, these restrictions are alleviated, rationalizing its increased ATPase activity. In conclusion, the crystallographic and single-molecule FRET data presented here established the precise nucleotide binding mode of and the conformational space available to the helicase-like domain of reverse gyrase. To guide future studies of the conformational changes upon ATP and DNA binding, further structural information about the complete *T. maritima* reverse gyrase is needed.

■ ASSOCIATED CONTENT

Supporting Information. Supplementary Figures S1 and S2; a structure-sequence comparison of the *A. fulgidus* and *T. maritima* reverse gyrase helicase-like domains and a multiple sequence alignment of reverse gyrase helicase-like domains highlighting the variability of the insertion region. This material is available free of charge via the Internet at http://pubs.acs.org.

■ AUTHOR INFORMATION

Corresponding Author

*Institute for Physical Chemistry, University of Muenster, Corrensstrasse 30, D-48149 Muenster, Germany. Phone: 0049-251 83 23421. Fax: 0049-251-83 29138. E-mail: dagmar.klostermeier@uni-muenster.de.

Funding Sources

This work was supported by the VolkswagenStiftung (D.K.) and the Swiss National Science Foundation (D.K.).

■ ACKNOWLEDGMENT

We thank the staff at SLS beamlines PX-II and PX-III for support during data collection.

■ REFERENCES

(1) Schoeffler, A. J., and Berger, J. M. (2008) DNA topoisomerases: Harnessing and constraining energy to govern chromosome topology. *Q. Rev. Biophys. 41*, 41–101.

(2) Gellert, M., Mizuuchi, K., O'Dea, M. H., and Nash, H. A. (1976) DNA gyrase: An enzyme that introduces superhelical turns into DNA. *Proc. Natl. Acad. Sci. U.S.A. 73*, 3872–3876.

(3) Kampmann, M., and Stock, D. (2004) Reverse gyrase has heat-protective DNA chaperone activity independent of supercoiling. *Nucleic Acids Res. 32*, 3537–3545.

(4) Hsieh, T. S., and Plank, J. L. (2006) Reverse gyrase functions as a DNA renaturase: Annealing of complementary single-stranded circles and positive supercoiling of a bubble substrate. *J. Biol. Chem. 281*, 5640–5647.

(5) Confalonieri, F., Elie, C., Nadal, M., de La Tour, C., Forterre, P., and Duguet, M. (1993) Reverse gyrase: A helicase-like domain and a type I topoisomerase in the same polypeptide. *Proc. Natl. Acad. Sci. U.S.A. 90*, 4753–4757.

(6) Declais, A. C., Marsault, J., Confalonieri, F., de La Tour, C. B., and Duguet, M. (2000) Reverse gyrase, the two domains intimately cooperate to promote positive supercoiling. *J. Biol. Chem. 275*, 19498–19504.

(7) Rodriguez, A. C., and Stock, D. (2002) Crystal structure of reverse gyrase: Insights into the positive supercoiling of DNA. *EMBO J. 21*, 418–426.

(8) Bouthier de la Tour, C., Amrani, L., Cossard, R., Neuman, K. C., Serre, M. C., and Duguet, M. (2008) Mutational analysis of the helicase-like domain of *Thermotoga maritima* reverse gyrase. *J. Biol. Chem. 283*, 27395–27402.

(9) Rodriguez, A. C. (2002) Studies of a positive supercoiling machine. Nucleotide hydrolysis and a multifunctional "latch" in the mechanism of reverse gyrase. *J. Biol. Chem. 277*, 29865–29873.

(10) Ganguly, A., Del Toro Duany, Y., Rudolph, M. G., and Klostermeier, D. (2011) The latch modulates nucleotide and DNA binding to the helicase-like domain of *Thermotoga maritima* reverse gyrase and is required for positive DNA supercoiling. *Nucleic Acids Res. 39*, 1789–1800.

(11) Del Toro Duany, Y., Jungblut, S. P., Schmidt, A. S., and Klostermeier, D. (2008) The reverse gyrase helicase-like domain is a nucleotide-dependent switch that is attenuated by the topoisomerase domain. *Nucleic Acids Res. 36*, 5882–5895.

(12) Del Toro Duany, Y., and Klostermeier, D. (2011) Nucleotide-driven conformational changes in the reverse gyrase helicase-like domain couple the nucleotide cycle to DNA processing. *Phys. Chem. Chem. Phys. 13*, 10009–10019.

(13) Jungblut, S. P., and Klostermeier, D. (2007) Adenosine 5′-O-(3-thio)triphosphate (ATPγS) promotes positive supercoiling of DNA by *T. maritima* reverse gyrase. *J. Mol. Biol. 371*, 197–209.

(14) Kabsch, W. (1988) Evaluation of single crystal X-ray diffraction data from a position sensitive detector. *J. Appl. Crystallogr. 21*, 916–924.

(15) Collaborative Computational Project, Number 4. (1994) The Collaborative Computational Project Number 4, suite programs for protein crystallography. *Acta Crystallogr. D50*, 760–763.

(16) McCoy, A. J., Grosse-Kunstleve, R. W., Adams, P. D., Winn, M. D., Storoni, L. C., and Read, R. J. (2007) Phaser crystallographic software. *J. Appl. Crystallogr. 40*, 658–674.

(17) Emsley, P., Lohkamp, B., Scott, W. G., and Cowtan, K. (2010) Features and development of Coot. *Acta Crystallogr. D66*, 486–501.

(18) Zwart, P. H., Afonine, P. V., Grosse-Kunstleve, R. W., Hung, L. W., Ioerger, T. R., McCoy, A. J., McKee, E., Moriarty, N. W., Read, R. J., Sacchettini, J. C., Sauter, N. K., Storoni, L. C., Terwilliger, T. C., and Adams, P. D. (2008) Automated structure solution with the PHENIX suite. *Methods Mol. Biol. 426*, 419–435.

(19) Esnouf, R. M. (1997) An extensively modified version of MOLSCRIPT that includes greatly enhanced coloring capabilities. *J. Mol. Graphics 15*, 132–134.

(20) Merritt, E. A., and Murphy, M. E. P. (1994) Raster3D Version 2.0: A program for photorealistic molecular graphics. *Acta Crystallogr. D50*, 869–873.

(21) Gouet, P., Courcelle, E., Stuart, D. I., and Metoz, F. (1999) ESPript: Analysis of multiple sequence alignments in PostScript. *Bioinformatics 15*, 305–308.

(22) Theissen, B., Karow, A. R., Kohler, J., Gubaev, A., and Klostermeier, D. (2008) Cooperative binding of ATP and RNA induces a closed conformation in a DEAD box RNA helicase. *Proc. Natl. Acad. Sci. U.S.A. 105*, 548–553.

(23) Gubaev, A., Hilbert, M., and Klostermeier, D. (2009) The DNA-gate of *Bacillus subtilis* gyrase is predominantly in the closed conformation during the DNA supercoiling reaction. *Proc. Natl. Acad. Sci. U.S.A. 106*, 13278–13283.

(24) Hilbert, M., Kebbel, F., Gubaev, A., and Klostermeier, D. (2010) eIF4G stimulates the activity of the DEAD box protein eIF4A by a conformational guidance mechanism. *Nucleic Acids Res. 39*, 2260–2270.

(25) Schütz, P., Bumann, M., Oberholzer, A. E., Bieniossek, C., Trachsel, H., Altmann, M., and Baumann, U. (2008) Crystal structure

of the yeast eIF4A-eIF4G complex: An RNA-helicase controlled by protein-protein interactions. *Proc. Natl. Acad. Sci. U.S.A. 105*, 9564–9569.

(26) Tanner, N. K. (2003) The newly identified Q motif of DEAD box helicases is involved in adenine recognition. *Cell Cycle 2*, 18–19.

(27) Tanner, N. K., Cordin, O., Banroques, J., Doere, M., and Linder, P. (2003) The Q motif: A newly identified motif in DEAD box helicases may regulate ATP binding and hydrolysis. *Mol. Cell 11*, 127–138.

(28) Andersen, C. B., Ballut, L., Johansen, J. S., Chamieh, H., Nielsen, K. H., Oliveira, C. L., Pedersen, J. S., Seraphin, B., Le Hir, H., and Andersen, G. R. (2006) Structure of the exon junction core complex with a trapped DEAD-box ATPase bound to RNA. *Science 313*, 1968–1972.

(29) Nielsen, K. H., Chamieh, H., Andersen, C. B., Fredslund, F., Hamborg, K., Le Hir, H., and Andersen, G. R. (2009) Mechanism of ATP turnover inhibition in the EJC. *RNA 15*, 67–75.

(30) Collins, R., Karlberg, T., Lehtio, L., Schutz, P., van den Berg, S., Dahlgren, L. G., Hammarstrom, M., Weigelt, J., and Schuler, H. (2009) The DEXD/H-box RNA helicase DDX19 is regulated by an α-helical switch. *J. Biol. Chem. 284*, 10296–10300.

(31) Sengoku, T., Nureki, O., Nakamura, A., Kobayashi, S., and Yokoyama, S. (2006) Structural Basis for RNA Unwinding by the DEAD-Box Protein *Drosophila* Vasa. *Cell 125*, 287–300.

(32) Kim, J. L., Morgenstern, K. A., Griffith, J. P., Dwyer, M. D., Thomson, J. A., Murcko, M. A., Lin, C., and Caron, P. R. (1998) Hepatitis C virus NS3 RNA helicase domain with a bound oligonucleotide: The crystal structure provides insights into the mode of unwinding. *Structure 6*, 89–100.

(33) Büttner, K., Nehring, S., and Hopfner, K. P. (2007) Structural basis for DNA duplex separation by a superfamily-2 helicase. *Nat. Struct. Mol. Biol. 14*, 647–652.

(34) Theis, K., Chen, P. J., Skorvaga, M., Van Houten, B., and Kisker, C. (1999) Crystal structure of UvrB, a DNA helicase adapted for nucleotide excision repair. *EMBO J. 18*, 6899–6907.

(35) Bourne, H. R., Sanders, D. A., and McCormick, F. (1990) The GTPase superfamily: A conserved switch for diverse cell functions. *Nature 348*, 125–132.

(36) Hilbert, M., Karow, A. R., and Klostermeier, D. (2009) The mechanism of ATP-dependent RNA unwinding by DEAD box proteins. *Biol. Chem. 390*, 1237–1250.

(37) Bono, F., Ebert, J., Lorentzen, E., and Conti, E. (2006) The crystal structure of the exon junction complex reveals how it maintains a stable grip on mRNA. *Cell 126*, 713–725.

(38) Caruthers, J. M., Johnson, E. R., and McKay, D. B. (2000) Crystal structure of yeast initiation factor 4A, a DEAD-box RNA helicase. *Proc. Natl. Acad. Sci. U.S.A. 97*, 13080–13085.

(39) Story, R. M., Li, H., and Abelson, J. N. (2001) Crystal structure of a DEAD box protein from the hyperthermophile *Methanococcus jannaschii*. *Proc. Natl. Acad. Sci. U.S.A. 98*, 1465–1470.

(40) Cheng, Z., Coller, J., Parker, R., and Song, H. (2005) Crystal structure and functional analysis of DEAD-box protein Dhh1p. *RNA 11*, 1258–1270.

(41) Brünger, A. T. (1992) Free R value: A novel statistical quantity for assessing the accuracy of crystal structures. *Nature 355*, 472–475.

(42) Laskowski, R. A., MacArthur, M. W., Moss, D. S., and Thornton, J. M. (1993) PROCHECK: A program to check the stereochemical quality of protein structures. *J. Appl. Crystallogr. 26*, 283–291.